

The Xian Shui He Fault system : deformation constrained by time serie analysis of Sentinel-1 data

L. Lemrabet (1), C. Lasserre (1), M.-P. Doin (2), A. Replumaz (2), P.H. Leloup (2), Sun Jianbao (3), M.L. Chevalier (4)

(1) Laboratoire de Géologie de Lyon, CNRS UMR 5570, (2) Université Grenoble-Alpes, ISTERre, Grenoble, France, (3) Institute of Geology, China Earthquake Administration, Beijing, China, (4) Key laboratory of Continental Tectonics and Dynamics, Institute of Geology, Chinese Academy of Geological Sciences.

INTRODUCTION

In eastern Tibet, the left-lateral, ~1400 km-long Xianshuihe fault system is one of the most tectonically active intra-continental fault system in China. More than 20 $M > 6.5$ earthquakes broke this fault since 1700, including the recent 2010 $M_w 6.9$ Yushu earthquake (fig. 1). We focus here on the Yushu - Ganzi - Xianshuihe active fault system (YGX), located on the eastern part of the Tibetan plateau. This left-lateral fault system accommodates part of the deformation related to the collision between the Indian and the Eurasian plates. Its Ganzi segment may represent a 350 km-long seismic gap, unbroken for the past ~120 years and capable of producing $M_w 7.6$ earthquakes. To measure the interseismic deformation across this area, we perform a time series analysis of 4 years of Sentinel-1 InSAR data. The objective of this study is to evaluate the YGX present-day behavior from InSAR measurements, its strike slip rate and degree of locking, to better assess seismic hazard in this region.

TECTONIC CONTEXT

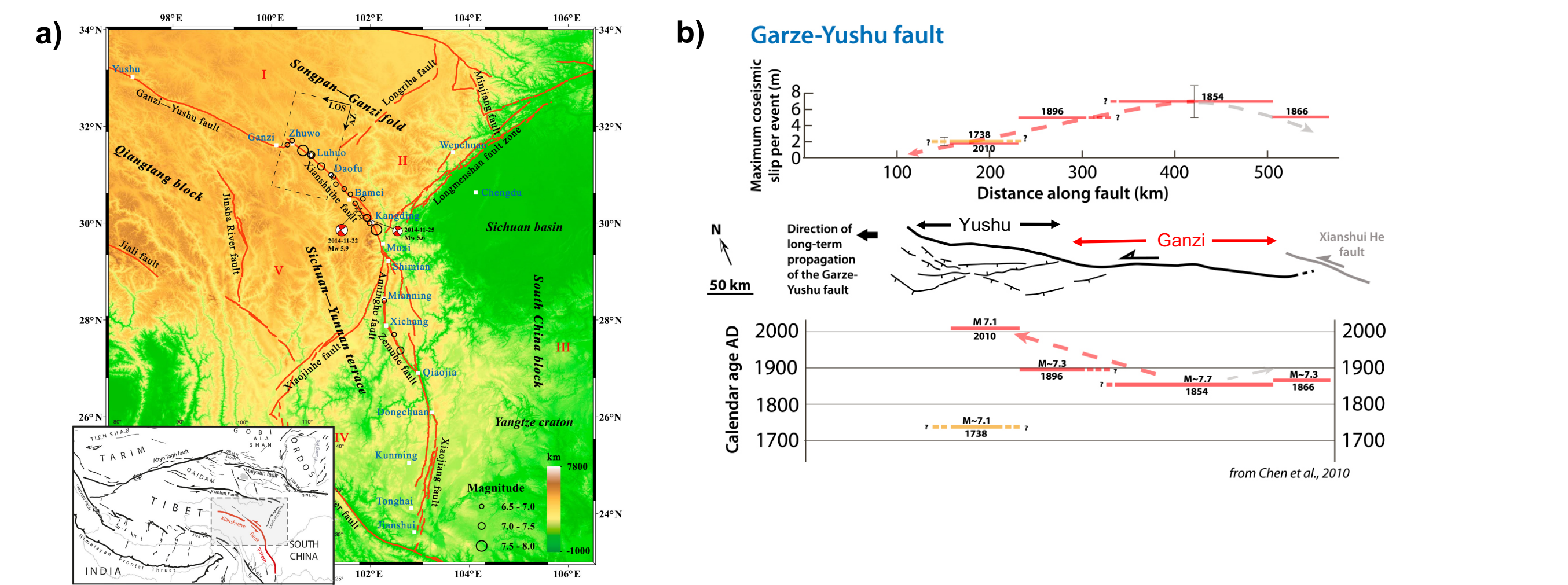


Figure 1 : a) Tectonic and topographic map in the eastern Tibetan Plateau and its surrounding regions, as well as historical earthquakes (black circles) of $M \geq 6.5$ since 1700 on the Xianshuihe fault system. The red lines denote the major faults. The study region is divided into five blocks (Modified from Jiang et al., 2015). b) Sequence of historical earthquakes and fault geometry, along Yushu and Ganzi segments (Modified from Perrin et al., 2016B)

SENTINEL-1 DATA SET

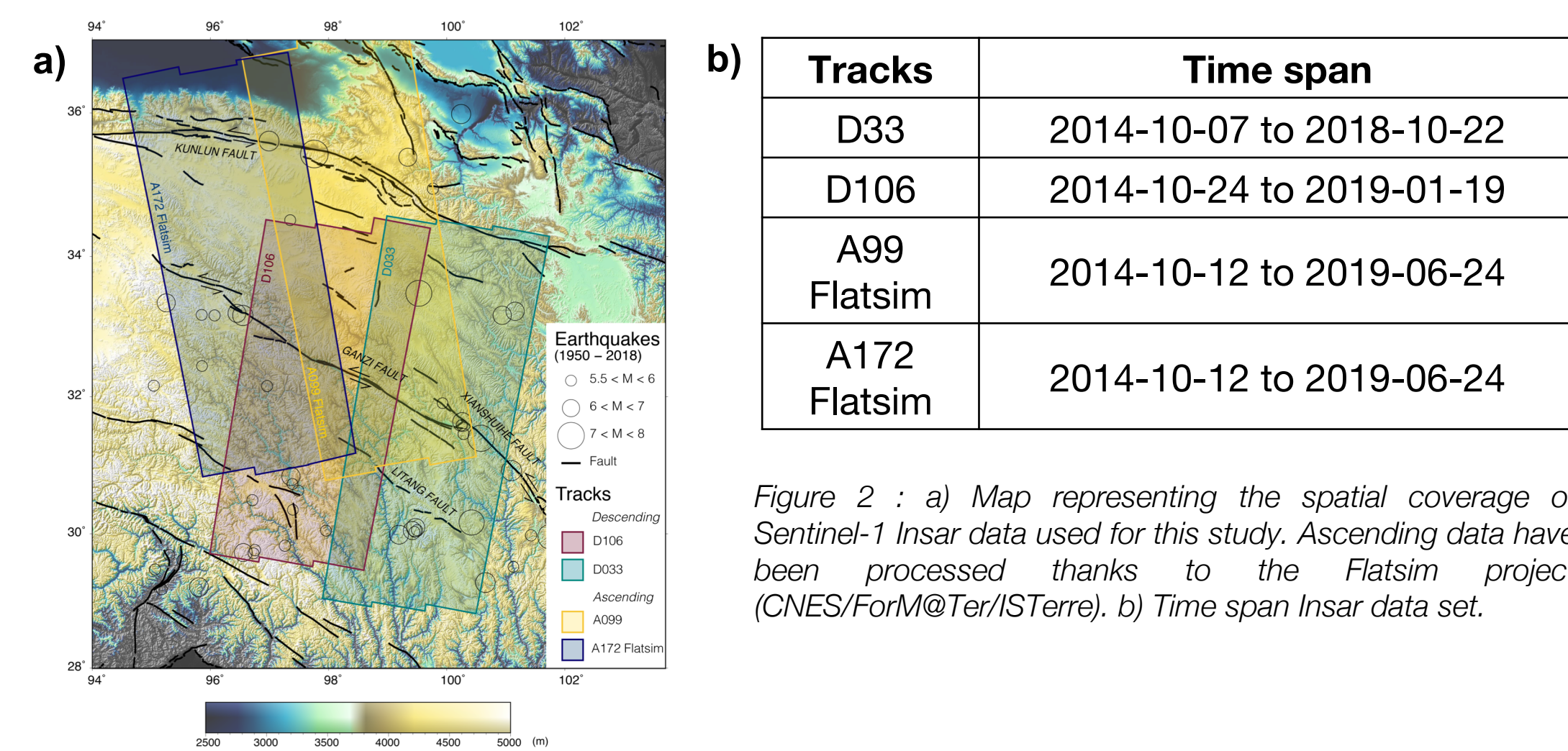


Figure 2 : a) Map representing the spatial coverage of Sentinel-1 InSAR data used for this study. Ascending data have been processed thanks to the Flatsim project (CNES/ForM@Ter/ISTERre). b) Time span InSAR data set.

INTERFEROGRAM NETWORK STRATEGY

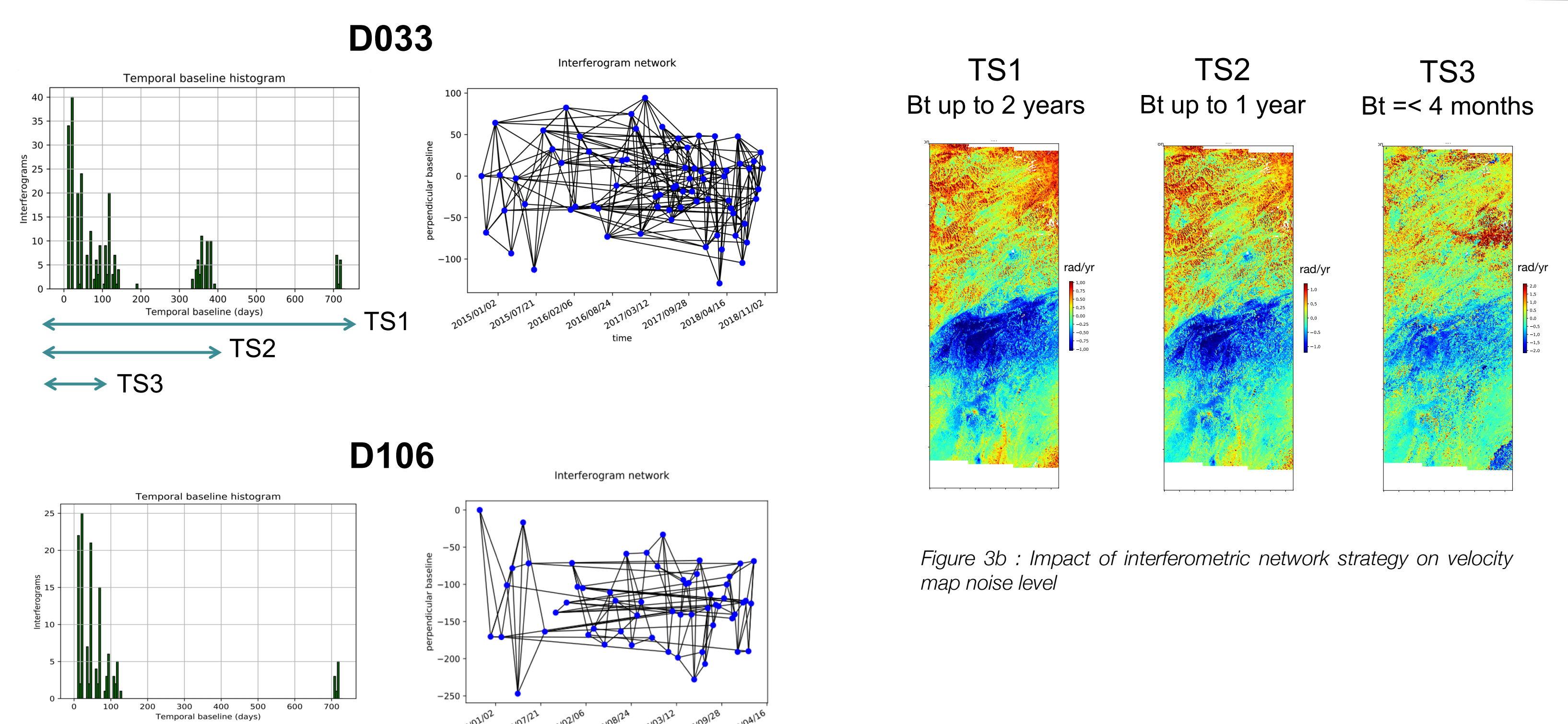


Figure 3a : Interferogram network and the temporal baseline histogram for the tracks D033 and D106.

TIME SERIES ANALYSIS

Time series analysis in overlapping regions of contiguous tracks in order to assess measurements quality

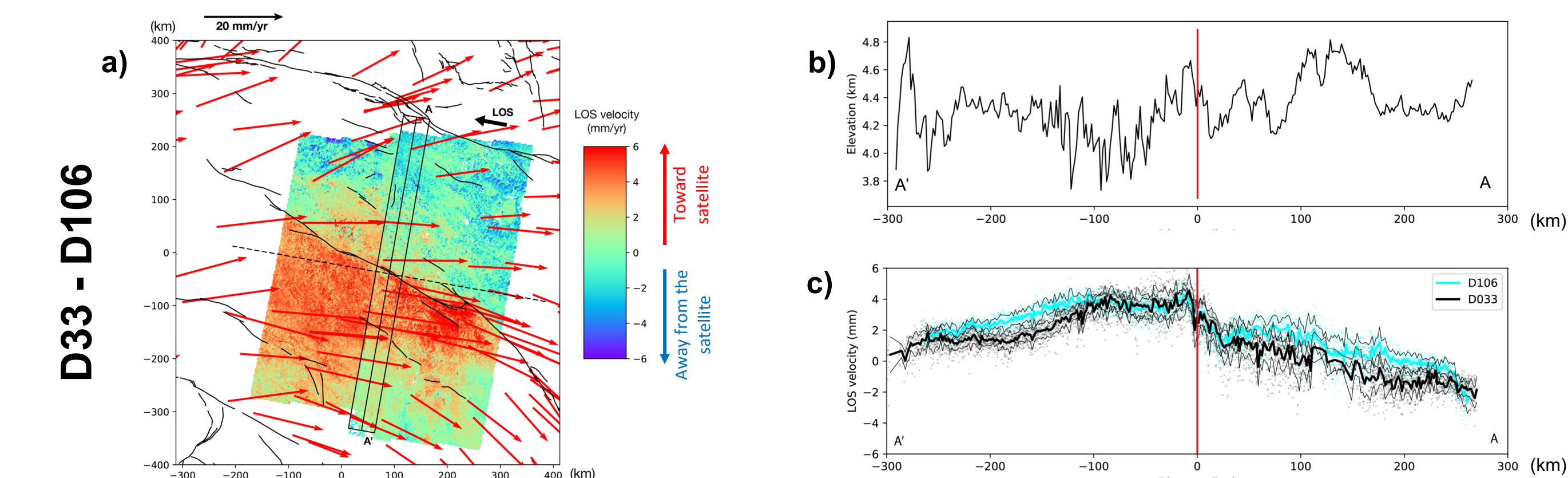


Figure 4 : Time series analysis of Ganzi section of XSH fault. (a) Line of sight velocity map. We use data located in the black rectangle, projected on the profile AA'. GPS data are represented by red arrows (Liang et al., 2013). (b) Average topography along profile AA'. (c) LOS velocities (black points) along profile AA', with average (black/blue lines for D033/D106) and standard deviation (black lines).

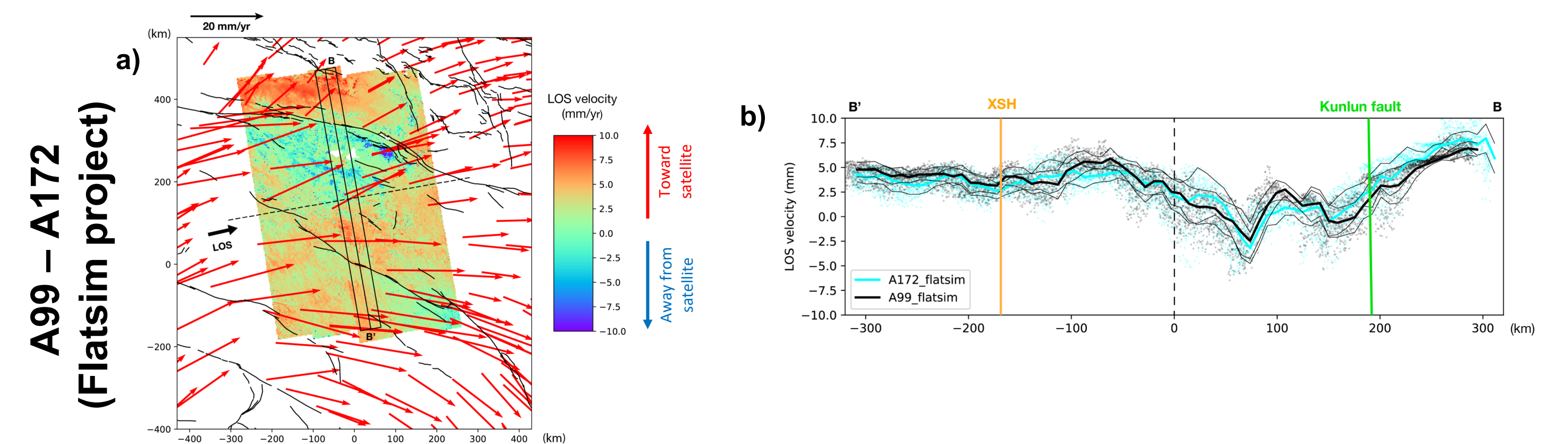


Figure 5 : Time series analysis for Ganzi section of XSH fault. (a) Line of sight velocity map. We use data located in the black rectangle, projected on the profile BB'. GPS data are represented by red arrows. (b) LOS velocities (black points) along the profile BB', with average (black/blue lines for A99/A172) and standard deviation (black lines).

Fault-perpendicular profiles on D106 and D33 tracks

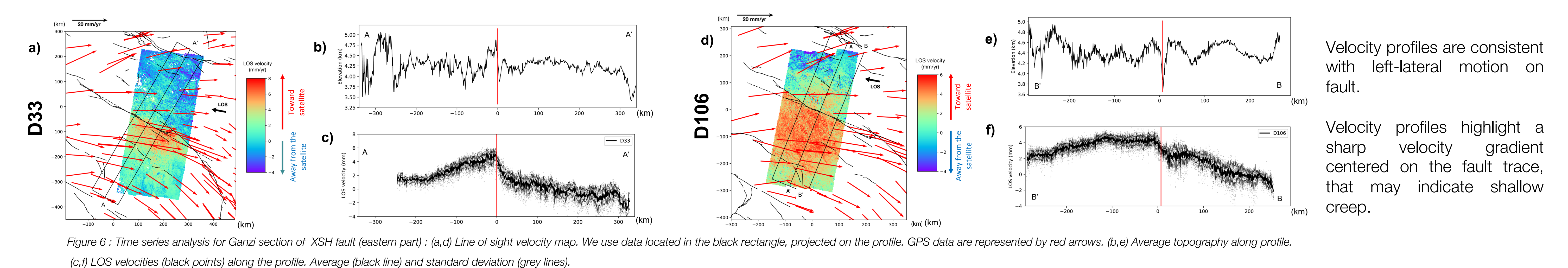


Figure 6 : Time series analysis for Ganzi section of XSH fault (eastern part) : (a,d) Line of sight velocity map. We use data located in the black rectangle, projected on the profile. GPS data are represented by red arrows. (b,e) Average topography along profile. (c,f) LOS velocities (black points) along the profile. Average (black line) and standard deviation (grey lines).

Velocity profiles are consistent with left-lateral motion on fault.

Velocity profiles highlight a sharp velocity gradient centered on the fault trace, that may indicate shallow creep.

MODELS

We use a Bayesian inversion of InSAR data based on Protools softwares from Daout et al. (2016). We invert velocity profiles perpendicular to the fault. We define a prior model of vertical, left-lateral fault in an elastic homogeneous half-space, with a uniform distribution of velocity (0-20 mm/yr) and locking depth (0-30 km).

The results suggest a slip rate of 4.8 ± 0.1 mm/yr and a locking depth of 3.3 ± 1.1 km on the eastern part of the Ganzi fault. However, the models suggest a slip rate of 5.7 ± 0.2 mm/yr and a locking depth of 28.0 ± 3.2 km on the western part of this segment.

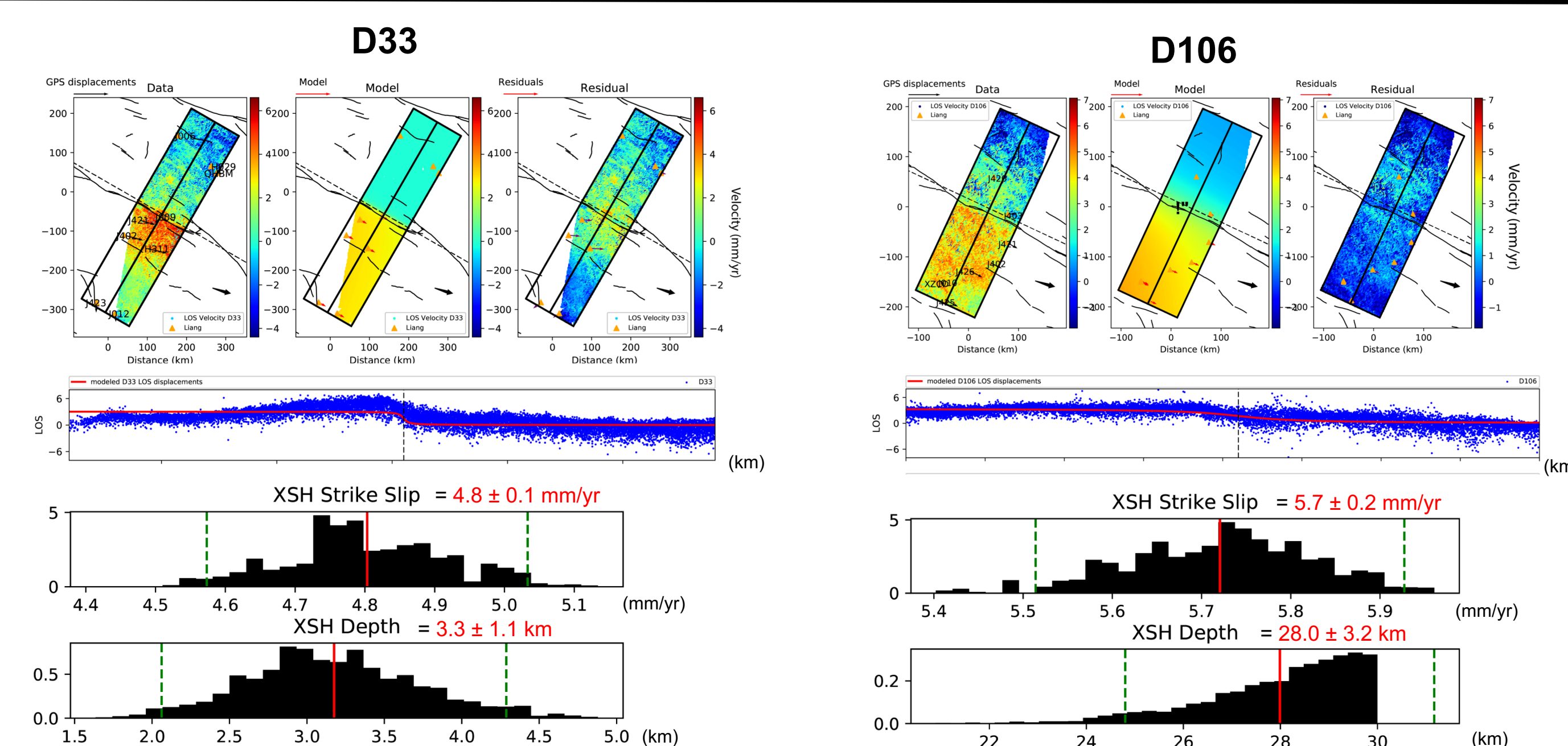


Figure 7 : Inversion results for fault-perpendicular profiles. Top : Data versus Model versus Residual, Middle : LOS velocity profiles (blue points) and model (red line), Bottom : Posterior probability density function (PDF) for velocity and locking depth.

COMPARISON

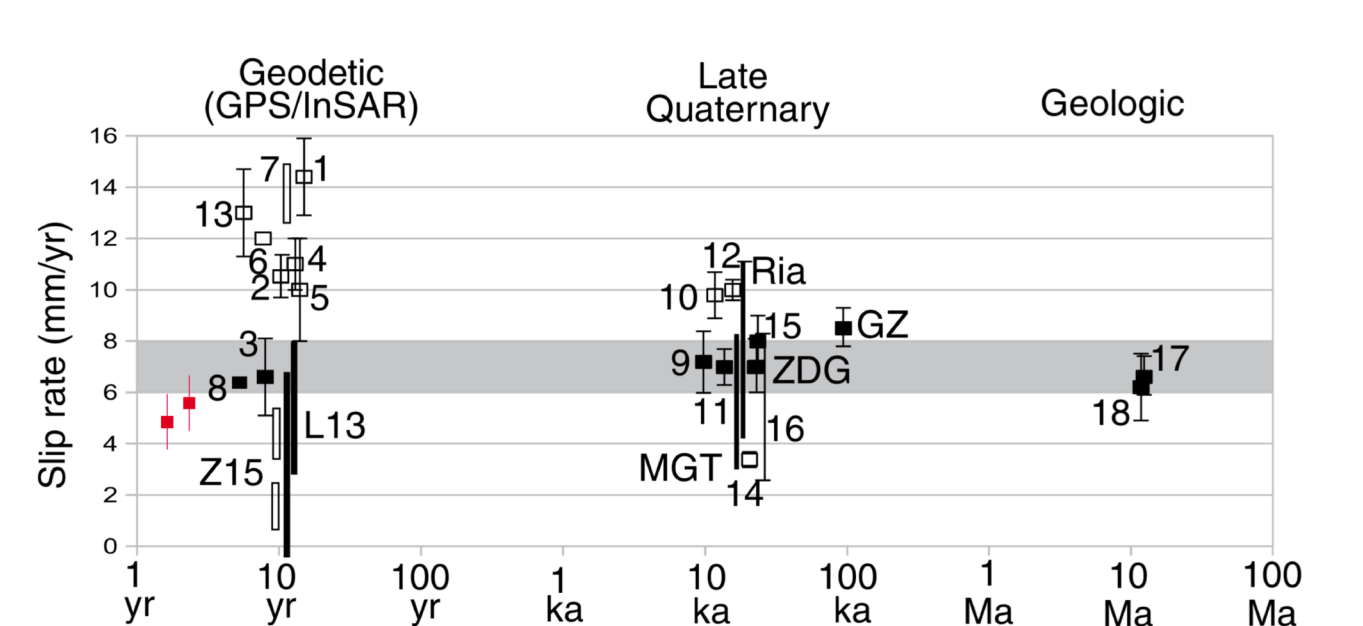


Figure 8 : Horizontal slip-rates from previous studies along the YGX fault at various timescales. Our results are rather consistent with other geodetic studies (modified from Chevalier et al., 2017).

CONCLUSION AND PERSPECTIVES

- We successfully performed time series analysis of Sentinel-1 images on selected tracks across the YGX, and retrieved the average Line of Sight velocity field across the fault.
- Quality measurements are assessed by comparison of LOS velocity in overlapping areas of processed tracks.
- Deformation localization is highlighted across major faults, with other off-fault deformation patterns related to tectonics or surface processes.

- Future work will include analysis of large-scale velocity maps produced through Flatsim project (CNES/ForM@Ter/ISTERre) and block models to account for relative block motions and elastic deformation across faults.

References

Chevalier, M. L., Leloup, P. H., Replumaz, A., Pan, J., Métis, M., Li, H., 2017. Temporally constant slip rate along the Ganzi fault, NW Xianshuihe fault system, eastern Tibet, Tectonophysics (accepted).

Doin, M.-P., Guillas, S., Jolivet, R., Lasserre, C., Lodge, F., Ducrest, G., Grandin, R., 2011. Presentation of the small-baseline NSBAS processing chain on a case example: the Etna deformation monitoring from 2003 to 2010 using ENVISAT data. Proceedings of the European Space Agency Symposium - Fringe -, Frascati, Italy.

Daout, S., R. Jolivet, C. Lasserre, M.-P. Doin, S. Barbot, P. Tapponnier, G. Peltzer, A. Socquet, Sun Jianbao, Along strike variations of the partitioning of convergence across the Haiyuan fault system detected by InSAR. Geophys. J. Int., 205 (1) : 536-547, doi : 10.1093/gjggw/028.

Grandin R., Interferometric processing of SLC Sentinel-1 TOPS data. Proceedings of the European Space Agency Symposium - Fringe -, Frascati, Italy.

Jiang, G., X. Xu, G. Chen, Y. Liu, Y. Fukahata, H. Wang, G. Yu, X. Tan, and C. Xu (2015). Geodetic imaging of potential seismogenic asperities on the Xianshuihe-Anninghe-Zemuhe fault system, southwest China, with a new 3-D viscoelastic interseismic coupling model. J. Geophys. Res. Solid Earth, 120, 1855–1873, doi:10.1002/2014JB011492.